JACS
JOURNAL OF THE AMERICAN CHEMICAL SOCIETY

Article

pubs.acs.org/JACS

Parahydrogen-Induced Polarization by Pairwise Replacement Catalysis on Pt and Ir Nanoparticles

Ronghui Zhou,[†] Evan W. Zhao,[†] Wei Cheng,[‡] Luke M. Neal,[‡] Haibin Zheng,[‡] Ryan E. Quiñones,[†] Helena E. Hagelin-Weaver,[‡] and Clifford R. Bowers*[,†]

[†]Department of Chemistry and [‡]Department of Chemical Engineering, University of Florida, Gainesville, Florida 32611, United States

Supporting Information

ABSTRACT: Pairwise and random addition processes are ordinarily indistinguishable in hydrogenation reactions. The distinction becomes important only when the fate of spin correlation matters, such as in parahydrogen-induced polarization (PHIP). Supported metal catalysts were not expected to yield PHIP signals given the rapid diffusion of H atoms on the catalyst surface and in view of the sequential stepwise nature of the H atom addition in the Horiuti−Polanyi mechanism. Thus, it seems surprising that supported metal hydrogenation catalysts can yield detectable PHIP NMR signals. Even more remarkably, supported Pt and Ir nanoparticles are shown herein to catalyze pairwise replacement on propene and 3,3,3-trifluoropropene. By simply flowing a mixture of parahydrogen and alkene over the catalyst, the scalar symmetrization order of the former is incorporated into the latter without a change in molecular structure, producing intense PHIP NMR signals on the alkene. An important indicator of the mechanism of the pairwise replacement is its stereoselectivity, which is revealed with the aid of density matrix spectral simulations. PHIP by pairwise replacement has the potential to significantly diversify the substrates that can be hyperpolarized by PHIP for biomedical utilization.

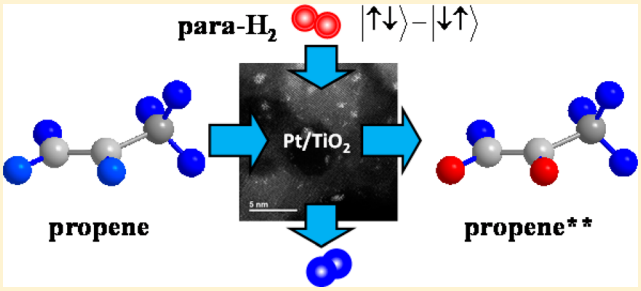

INTRODUCTION

Significant breakthroughs in the methodology of nuclear spin hyperpolarization have stimulated a renaissance in NMR spectroscopy and imaging in recent years. Driven mainly by biomedical applications, hyperpolarization techniques help to overcome the inherently low sensitivity of conventional NMR, which stems from the typically unfavorable Boltzmann distribution among the nuclear spin energy levels.[1] Parahydrogen-induced polarization (PHIP)[2−8] is a simple, robust, inexpensive, and scalable technique for rapid and continuous production of bulk quantities of hyperpolarized liquids and gases. The pure symmetrization order inherent in the protons of parahydrogen (p-H_2) is transformed via a symmetry-breaking chemical hydrogenation reaction into NMR-observable hyperpolarization. However, the PHIP effect is entirely absent unless the hydrogenation occurs in a pairwise fashion; i.e., both H atoms must originate from the same H_2 molecule. In theory, nuclear spin hyperpolarization on the order of unity is attainable by PHIP, affording high-field, room-temperature NMR signal enhancements of over 4 orders of magnitude.[3,7]

Following its prediction[2] and first observation,[3] PHIP NMR evolved into a unique tool for the elucidation of mechanisms of homogeneous hydrogenation reactions catalyzed by transition-metal complexes in solution.[4,6,9−12] A surge of interest in PHIP has been stimulated by important recent developments, which include the preparation of hyperpolarized biomolecular agents for diagnostic magnetic resonance imaging[13−16] and signal amplification by reversible exchange (SABRE),[8,17] a non-hydrogenative form of PHIP. In a step toward production of catalyst-free hyperpolarized species for biomedical utilization, PHIP has recently been achieved in hydrogenations over immobilized Ir,[18,19] Au,[20] and Rh[21] complexes. The present work is inspired by the demonstration of PHIP using oxide-supported metal nanoparticle catalysts (hetPHIP).[18,22−27] Supported metals are used extensively in industrial hydrogenation and offer important advantages over homogeneous catalysis, including ease of separation of the product and compatibility with a continuous-flow reactor configuration. Recent advances in this direction include stopped-flow imaging using hyperpolarized propane gas prepared by hetPHIP.[28,29] Indicating that a SABRE-like effect can also be achieved using these catalysts, ref 27 presented hyperpolarized 1-octene signals obtained in the hydrogenation of 1-octene (the reactant) with para-enriched H_2 over a Rh/TiO_2 catalyst. The specific mechanism for the substrate signal enhancement was not identified in this preliminary observation, but it has been investigated further using deuterated propene in a recent study by the same authors.[28]

Received: November 7, 2014
Published: January 15, 2015

DOI: 10.1021/ja511476n
J. Am. Chem. Soc. 2015, 137, 1938−1946

Herein we report intense propene (and trifluoropropene) PHIP signals that result when mixtures of these gases with parahydrogen are passed through a reactor bed containing supported Pt or Ir nanoparticles. In this SABRE-like pairwise replacement (PR) PHIP effect, two unpolarized protons of the substrate are replaced with two protons originating from the same parahydrogen molecule, resulting in the incorporation of symmetrization order into the substrate with no change in its chemical structure. Furthermore, we propose a specific mechanism underpinning this PR-PHIP effect that is critical to its further generalization and optimization. PR-PHIP using supported metal nanoparticle catalysts could potentially broaden the scope of substrates that can be hyperpolarized by this class of catalyst.

BACKGROUND

Most aspects of heterogeneous hydrogenation of olefins over supported metals are explained by the Horiuti–Polanyi (HP) mechanism,[30] illustrated in Figure 1. Hydrogen molecule

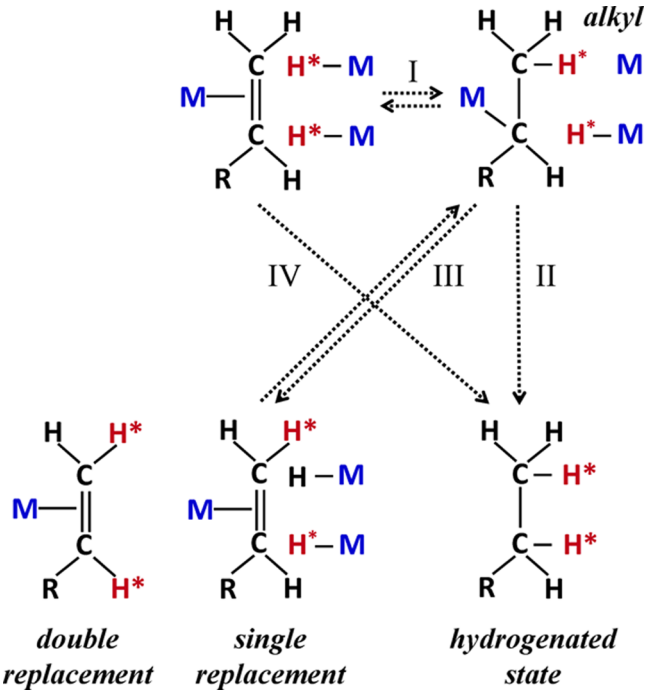

Figure 1. Alkene hydrogenation and exchange on a metal catalyst M, according to the HP mechanism (π-bonding representation) (ethene, R = H; propene, R = CH_3). * represents a spin label. In the original HP mechanism, * = deuterium.[30] In the context of PHIP, * indicates a proton in a spin-correlated proton pair (e.g., a singlet-state). Hence, PHIP-hyperpolarized propene is denoted propene**. Recent spectroscopic studies[37] suggest a π-bonded form of the adsorbed alkene as opposed to the di-σ structure. Steps I + III yield the single replacement state. The double replacement state can be reached by iteration of steps I + III or by the PR mechanism described in the text. Step IV is referred to as direct saturation.

dissociation is followed by sequential addition of hydrogen atoms to the substrate (steps I + II). The reversibility of the β-hydride transfer/elimination (step I) accounts for incorporation of multiple deuterium atoms into the alkene and alkane.[31] The *double replacement state* shown in Figure 1 can be achieved by two iterations of steps I + III. Using improved instrumentation, the pattern of deuteration in the alkane and alkene resulting from deuterium addition and exchange over Al_2O_3-supported Pt and Pd was examined by Bond.[32] Consistent with the HP mechanism, reactions of ethene with D_2 yield HD and C_2H_3D as well as more extensively exchanged ethenes and ethanes containing zero to six deuterium atoms. However, a careful statistical analysis of the deuterium distribution in the products indicated that the amount of $C_2H_4D_2$ in the products was disproportionately high and could not be accounted for by sequential addition alone. Thus, Bond postulated a *direct saturation* step (step IV in Figure 1),[31,32] a pathway that preserves the spin-correlation inherent in H_2. Direct saturation might occur at specific "zero-dimensional" active sites for pairwise addition, which have been inferred from the metal particle size dependence of the pairwise selectivity over Pt.[23] Evidence suggests low coordination metal atoms located at edges or kink atoms on the metal cluster which bind molecular H_2.[23,24] Pairwise addition at such sites could conceivably occur by a Eley–Rideal mechanism, invoked in the older literature on reactions catalyzed by other group 8–10 metals,[31] where an H_2 molecule reacts with an adsorbed species without dissociating first. Recent theoretical and experimental work indicates that hydrogenation catalysis on the relatively inert group 11 metals (i.e., Cu, Ag, and Au) that do not activate H_2 due to the high dissociation barrier occurs by a non-HP mechanism in which molecular hydrogen directly reacts with substrates.[33,34] Such a reaction pathway would be favorable for the pairwise dihydrogen addition, a primary requirement to observe the PHIP effect.

There are two distinct variations of PHIP: PASADENA (*p*arahydrogen *a*nd *s*ynthesis *a*llow *d*ramatically *e*nhanced *n*uclear *a*lignment)[2,3] and ALTADENA (*a*diabatic *l*ongitudinal *t*ransport *a*fter *d*issociation *e*ngenders *n*et *a*lignment).[5] In the PASADENA effect, both the hydrogenation reaction and NMR detection are carried out entirely at high magnetic field, yielding signals that are maximized in the weak spin-coupling regime. In ALTADENA, hydrogenation is carried out at low magnetic field, where the two protons remain strongly coupled after addition, followed by rapid but sufficiently "adiabatic" transport to high field, where the spin-$^1/_2$ pair may be weakly coupled, depending on the substrate. An important difference between PASADENA and ALTADENA is the possibility of sharing scalar order among spins in a strongly coupled network at low (or zero) magnetic field. Such sharing forms the basis for the SABRE effect, first demonstrated using the complex $[Ir(H)_2(PCy_3)(substrate)_3][BF_4]$ to bind pyridine in the solution state.[8] The Ir complex simultaneously binds both pyridine and H_2 as a dihydride, and pyridine nuclei become hyperpolarized via coherence transfer within the complex. Silica-immobilized Ir[19] and Rh[21] complexes appear to show SABRE-like PR-PHIP signal enhancements at high magnetic field under PASADENA conditions, indicating that the sharing of polarization occurs through a chemical exchange mechanism rather than by coherence transfer.

We have chosen to focus on the Pt/TiO_2 system in the present work because this combination of metal and support is known to be a highly active catalyst for hydrogenation of double and triple bonds.[24,35] The high activity has been attributed to strong metal support interactions (SMSI) on TiO_2.[26,35] These SMSI can lead to migration of TiO_x ($x < 2$) over the surface of the metal particles when catalysts are reduced in H_2 at elevated temperatures,[36] and hydrogenation could conceivably occur at the interface of Pt and TiO_2 (e.g., on Pt–O bonds). The fact that pure TiO_2 without an active metal

DOI: 10.1021/ja511476n
J. Am. Chem. Soc. 2015, 137, 1938–1946

Table 1. Metal Loading, Chemisorption Data, Percent Dispersion, and Estimated Average Particle Size for Select Catalysts Used in This Work

			H_2 chemisorption			CO chemisorption		
name	catalyst	loading, wt %	V_{gc}, μL/g	% dispersion	size, nm	V_{gc}, μL/g	% dispersion	size, nm
CAT17	Pt/TiO_2	0.76	560	130	0.7	700	80	1.2
CAT23	Pt/TiO_2	0.72				730	90	1.1
CAT18	Ir/TiO_2	0.54	250	80	1.0	500	80	1.0

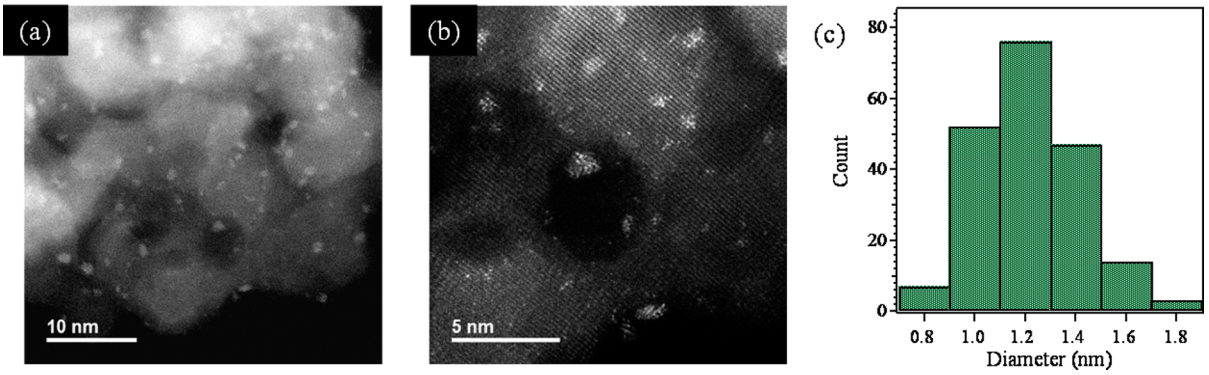

Figure 2. STEM images of the Pt/TiO_2 catalyst (a) at low magnification and (b) at high magnification. (c) Histogram of Pt particles sizes based on the analysis of 200 particles.

is not an active catalyst in this reaction was confirmed by running the reaction over the pure TiO_2 support. To isolate the possible role of the oxide support on the PR process, PHIP experiments were also performed using both Pt/Al_2O_3 and Pt/SiO_2, since Al_2O_3 and SiO_2 are regarded as neutral, non-interacting supports.[36] Iridium is included in our study to explore the generality of the SABRE-like signal amplification in another metal. To our knowledge, PHIP using Ir nanoparticles has not been previously reported.

EXPERIMENTAL SECTION

Catalyst Synthesis. Two Pt/TiO_2 batches (referred to as CAT17 and CAT23), an Ir/TiO_2 catalyst, and a Pt/Al_2O_3 catalyst were prepared by the *precipitation–deposition* (PD) method (see the Supporting Information), all with a nominal loading of 1%. Actual weight percentage loadings, as measured by ICP-AES, are reported in Table 1. Additionally, 1% Pt/TiO_2 and 1% Pt/SiO_2 catalysts were prepared by a modified impregnation method, as described in the Supporting Information. All of these catalysts demonstrated strong PHIP and PR-PHIP signals.

Metal Surface Area. Pt and Ir metal loadings were quantified by inductively coupled plasma-atomic emission spectrometry (ICP-AES). Active metal surface area was measured by both CO and H_2 chemisorption titration, as described in the Supporting Information. An estimation of the Pt and Ir average particle sizes was afforded by combining the volumes of adsorbed CO or H_2 with the metal loadings determined by ICP-AES. Details are given in the Supporting Information. The metal loading, chemisorption data, dispersion, and estimated average particle size for select catalysts used in this work are summarized in Table 1.

Note that the metal dispersion measured by H_2 chemisorption exceeds 100%, possibly due to a spillover effect or chemisorption of more than one H atom per platinum surface atom, as has been reported in the literature.[38] Therefore, the Pt particle size obtained from the H_2 chemisorption data is considered to be underestimated.

Scanning Transmission Electron Microscopy (STEM). Representative micrographs of the Pt/TiO_2 catalysts are shown in Figures 2 and S1 (Supporting Information). These STEM images were collected on a probe aberration corrected JEOL JEM-ARM200cF with a cold field emission electron gun. The STEM high-angle annular dark-field (HAADF) image was recorded with the JEOL HAADF detector using the following experimental conditions: probe size 7 c, CL aperture 30 μm, scan speed 32 μs/pixel, and camera length 8 cm (which corresponds to a probe convergence semiangle of 11 mrad and collection angles of 76–174.6 mrad). The STEM resolution of the microscope is 0.78 Å. The intensity of atomic columns in STEM HAADF images is proportional to Z^n, where Z is the atomic number and n is close to 2, and has a monotonic relationship to sample thickness.[39] Due to the large difference in atomic number, the Pt particles are seen as bright areas against the darker TiO_2 background. The presence of Pt on the TiO_2 support was confirmed by energy-dispersive X-ray spectroscopy (Figure S2, Supporting Information).[40]

A histogram of the Pt particle diameters, shown in Figure 2c, was constructed by analysis of the STEM images using the ImageJ[41] image analysis software. Isolated single Pt atoms were not included, as they may easily migrate to the large particles under reaction conditions. On the basis of the statistics of 200 particles, the average Pt particle size is found to be 1.1 nm with a standard deviation of 0.2 nm, in good agreement with the size estimation obtained by CO chemisorption titration and somewhat larger than the value obtained from the H_2 chemisorption titration.

Substrates. Propene was purchased from Airgas, Inc. (99.5% purity), and 3,3,3-trifluoropropene (purity 99%) was purchased from Synquest Laboratories (Alachua, FL). The gases were stored in the earth's field; therefore, all nuclear spins on the substrate are initially unpolarized.

ALTADENA Flow Reactor System. The solid catalyst was packed into a 1/4 in. o.d. U-shaped glass tube mounted inside a ceramic heating element inside which the temperature of the catalyst bed can be varied from ~25 to 400 °C. The reactor is mounted just above the bore opening of a 9.4 T Bruker Ultrashield actively shielded magnet, where the fringe field is 5 mT. The temperature of the reactor bed is monitored using a K-type thermocouple probe inserted directly into the bed. A continuous stream of H_2 gas, enriched to approximately 50% in the parahydrogen spin isomer (hereafter referred to as p-H_2), is produced on demand by passing normal hydrogen (n-H_2, an approximate 1:3 mixture of p-H_2 and ortho-H_2, o-H_2) through a 1/4 in. copper coil filled with activated charcoal and submerged in liquid N_2 (77 K). The parahydrogen fraction was confirmed by NMR. Mixtures containing H_2 (normal or para-enriched), propene, and N_2 are prepared using three separate mass flow controllers (Alicat Scientific, Inc.). The reactant gas mixture is delivered to the reactor

DOI: 10.1021/ja511476n
J. Am. Chem. Soc. 2015, 137, 1938–1946

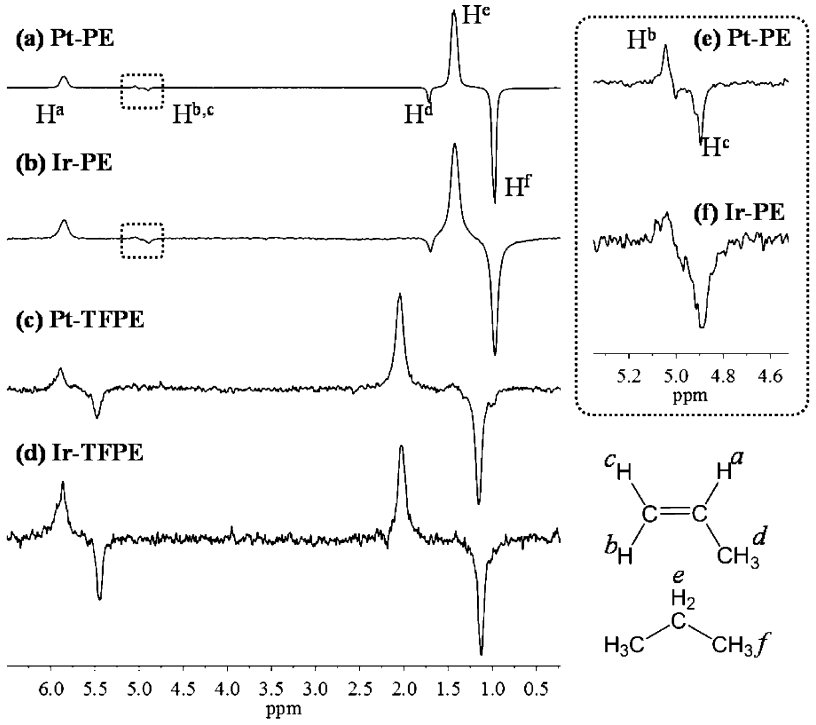

Figure 3. ALTADENA proton NMR spectra of the effluent from the hydrogenation reactor containing 10 mg of either Pt/TiO_2 or Ir/TiO_2 catalysts at a reactor temperature of 300 °C. (a, b) Propene (PE) was used as substrate. (c, d) Trifluoropropene (TFPE) was used as substrate. The inset shows an expansion around the CH and CH_2 peaks of PE and TFPE. The peaks labeled a–f correspond to the structures shown at bottom right.

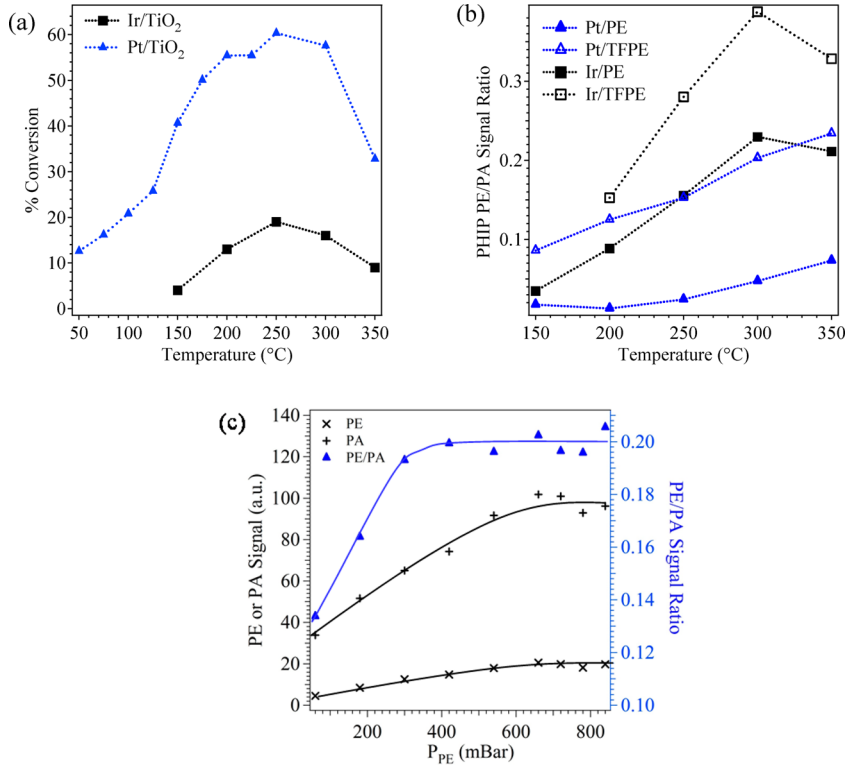

Figure 4. (a) Reaction temperature dependence of the total conversion (eq 1) of propene (PE) to propane (PA) on Ir/TiO_2 and Pt/TiO_2 nanoparticle catalysts. (b) Reaction temperature dependence of the alkene/alkane ALTADENA signal ratio obtained using the Pt/TiO_2 and Ir/TiO_2 catalysts. (c) Propene and propane ALTADENA signals and signal ratio (blue triangles, right axis) acquired over Pt/TiO_2 at 300 °C at a series of propene partial pressures with fixed p-H_2 pressure and constant total pressure (by adjusting the N_2 pressure) at a total flow rate of 400 mL/min (see Figure S7, Supporting Information).

inlet using 1/16 in. i.d. (1/8 in. o.d.) PFA tubing. Gases were transported from the outlet of the reactor U-tube to the bottom of a 10 mm medium wall thickness NMR tube via 1/16 in. i.d. PFA tubing that passes through the center of a larger diameter (1/4 in. o.d., 1 m

DOI: 10.1021/ja511476n
J. Am. Chem. Soc. 2015, 137, 1938–1946

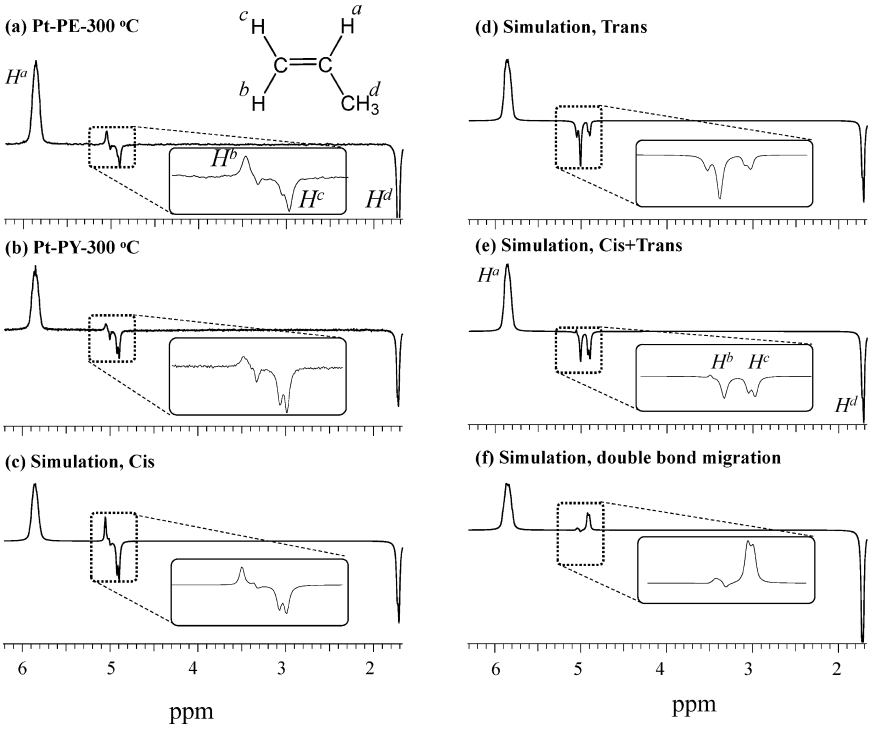

Figure 5. (a, b) Experimental ALTADENA difference spectra acquired with the Pt/TiO_2 (10 mg) catalyst at 300 °C using propene (PE) and propyne (PY), respectively. (c, d) Six-spin SpinDynamica spectral simulations assuming syn- and anti-addition, respectively. (e) Simulated spectrum resulting from equal amounts of syn and anti pairwise replacement. (f) Simulated spectrum resulting from double bond migration following pairwise replacement. In both the experiments and simulations, the RF pulse flip angle is 78°.

length) stainless steel tube that is connected to the NMR tube with a Swagelok fitting. The NMR tube is positioned within a standard Bruker Biospin 10 mm liquids probe.

Heterogeneous Hydrogenation in the Gas Phase at Low Field. Catalysts were loaded into the glass U-tube. Prior to reactions, catalysts were reduced in pure H_2 atmosphere at elevated temperature (170 °C for Pt and 350 °C for Ir) for 30 min at a flow rate of 200 mL/min followed by N_2 purging. During reactions, streams of N_2, H_2, and propene at flow rates of 260, 120, and 20 mL/min, respectively, were mixed together and delivered to the reactor. At the total flow rate of 400 mL/min, the transport time from the reactor outlet to the NMR probe is about 0.5 s. The propene conversion was calculated from the thermally polarized integrated signals on the alkene and alkane, after correcting for incomplete relaxation in the magnetic field at the flow rate of 400 mL/min, using eq 1:

$$\text{conversion} = \frac{S_{CH_2}(\text{propane})/2}{S_{CH_2}(\text{propane})/2 + S_{CH}(\text{propene})} \quad (1)$$

NMR Spectroscopy. Spectra of the flowing reactor effluent were acquired on a Bruker Avance 400 MHz (B_0 = 9.4 T) NMR spectrometer. ALTADENA and thermally polarized NMR signals were signal-averaged using a 17 μs 78° pulse,[42] an eight-step phase cycle, and a recycle delay of 2 s. The ALTADENA difference spectra presented in Figure 3 were obtained by subtraction of the spectra acquired with n-H_2 (see Figure S3, Supporting Information) from the spectra acquired with p-H_2. The residual peak due to the orthohydrogen content of the unreacted H_2, which is different for para-enriched H_2 and n-H_2, was removed from the difference spectrum by incorporation into the cubic spline baseline correction.

RESULTS AND DISCUSSION

First, we consider what happens when the reactant gas mixture contains n-H_2 (a 3:1 mixture of orthohydrogen and parahydrogen) and substrate. Hydrogenation adducts are formed with unpolarized proton spins, regardless of whether the addition is pairwise or random. As the reaction products flow into the high magnetic field of the superconducting NMR magnet, NMR-observable proton magnetization develops by thermal equilibration. At the experimental flow rate of 400 mL/min, the proton relaxation on propene and propane at the time it is detected by NMR is about 15−20% complete.

Thermally polarized spectra of propane resulting from hydrogenation of propene with n-H_2 at 300 °C yields CH_2 and CH_3 peaks with areas in the expected 1:3 ratio (see Figure S3a,b of the Supporting Information). Due to the lower conversion obtained for TFPE, the thermally polarized signals for this substrate are at, or below, the level of the noise (Figure S3c,d, Supporting Information). In propene, the integrated signals for CH, CH_2, and CH_3 signals are observed in the expected 1:2:3 ratio, all in the absorption phase. The temperature dependence of the conversion, calculated from the thermally polarized propane and propene peak areas using eq 1, is plotted in Figure 4a. Conversions to propane were found to be highly reproducible in a set of four different Pt/TiO_2 preparations synthesized with the same Pt loading. The Pt/TiO_2 catalyst delivers significantly higher conversion, peaking at about 60% at 250 °C, while the conversion over Ir peaks at about the same temperature but reaches only 20%. Conversions for TFPE could not be estimated due to an insufficient thermally polarized signal (see Figure S3c,d, Supporting Information). Low conversions resulted from high flow rates and the small amount of catalyst used in the experiments.

Reactions with p-H_2 yield spectra that can be decomposed into contributions originating from ordinary thermal Zeeman order and ALTADENA scalar order. However, scalar order is created only if p-H_2 is incorporated into the substrate in a pairwise fashion. Substrate molecules formed by random

DOI: 10.1021/ja511476n
J. Am. Chem. Soc. 2015, 137, 1938−1946

addition or random replacement are initially unpolarized but acquire thermal Zeeman order upon transport to high field. As noted in the Experimental Section, the pure ALTADENA spectra shown in Figure 3a–d were obtained by subtracting the spectra acquired with n-H_2 from those acquired with p-H_2. The ALTADENA net alignment signal patterns are observed on the hydrogenation adduct propane with a S_{CH_2}:S_{CH_3} peak area ratio close to 1:1. Similar (though less intense) ALTADENA signals were observed when hydrogenation was carried out over Ir/SiO_2, Pt/SiO_2, or Pt/Al_2O_3 (see Figure S4, Supporting Information).

In addition to hyperpolarized propane, unanticipated ALTADENA signal enhancements are also observed on all protons of propene, *the reactant*. The enhanced propene peaks obtained with Pt/TiO_2 are labeled a–d in the spectra shown in Figure 3. The Ir/TiO_2 catalyst and Pt on the other supports (i.e., Al_2O_3 and SiO_2) produced similar signals (see Figure S4, Supporting Information). Because these signals were not expected, we initially suspected that the anomalous ALTADENA signals might originate from hydrogenation of alkyne present as an impurity in the stock propene. However, GC/MS analysis of the stock propene gas (Airgas, Inc.; see Supporting Information) shows that the concentration of propyne, if it is even present, is below the detection limit, establishing an upper bound on the propyne impurity molar fraction of less than 300 ppm. The stock propene gas was also analyzed by high-resolution solution-state ^{1}H NMR by dissolution in DMSO-d_6. Even though propyne is more soluble than propene in this solvent, no trace of any propyne is detected, despite a s/n ratio >100 for the propene CH signal (see Figure S5, Supporting Information). We observed similar ALTADENA signals in TFPE from a different gas cylinder and different manufacturer. Therefore, we unequivocally rule out the possibility that the anomalous PHIP signals are derived from pairwise addition to trace levels of propyne contained in the stock propene gas.

The temperature dependence of the alkene:alkane ALTADENA signal ratios obtained over the Pt/TiO_2 and Ir/TiO_2 catalysts using normal and fluorinated propene is shown in Figure 4b. The signal ratios increase with temperature, and the ratio is highest for the fluorinated alkene substrate. The highest propene/propane signal ratio (c.a. ∼0.4) was observed with the Ir/trifluoropropene metal/substrate combination at 300 °C. The dependence of the propene and propane signals and signal ratio on propene partial pressure is presented in Figure 4c. The CH_3 ALTADENA signal enhancement relative to the thermally polarized CH_3 signal (per proton) increased monotonically from about 25 at P_{PE} = 60 mbar to 50 at 300 mbar, where it plateaued. The greater significance of these trends is discussed below.

As to the origin of the SABRE-like ALTADENA signals, an important clue is revealed by comparing the propene region of the NMR spectra resulting when p-H_2 reacts with either propene or propyne over Pt/TiO_2 catalyst at 300 °C, as shown in parts a and b of Figure 5, respectively. Clearly, the two spectra bear a close resemblance. In both, the unresolved cis doublets (H^c) appear in emission, while the trans doublet (H^b) appears with partial absorption/partial emission phase. As noted above, ALTADENA scalar order spreads through the molecule via the scalar coupling network at low field, which explains why the methyl protons (H^a), which did not originate as H_2, exhibit an intense ALTADENA signal. In complex *J*-coupling networks containing many spins, prediction of the phase and amplitude of the ancillary multiplet signals can be nontrivial, and spectral interpretation by inspection is not feasible. Here, assessment of the stereoselectivity of the pairwise addition based on the spectrum of the cis and trans signals is facilitated by density operator/matrix simulations of the spin dynamics. SpinDynamica[43] density operator simulation of the propene ALTADENA spectrum resulting from stereoselective syn- and anti-addition to propyne are presented in parts c and d of Figure 5, respectively (see Supporting Information for simulation details). The cis and trans dispositions of the scalar order give strikingly different ALTADENA spectra. Nonstereoselective addition is simulated by averaging the two spectra (Figure 5e). The ALTADENA simulations of pairwise replacement immediately followed by double bond migration is shown in Figure 5f. Clearly, the experimental ALTADENA spectrum most closely resembles the simulated syn-addition spectrum. The strong emission phase of H^c observed in the experimental spectrum indicates that the signal contribution from molecules having undergone double bond migration is relatively minor. Propene formed by pairwise hydrogenation of propyne exhibits similar syn-addition stereoselectivity under these same reaction conditions.

Deuterium exchange studies with alkanes and alkenes on alumina-supported Pt and Ir have shown that the extent of exchange depends on the metal, substrate chemistry, and reaction conditions.[31,32] Each of these factors is investigated in the present work. Deuterium exchange was found to increase with rising temperature.[31] Paralleling this trend, our propene/propane ALTADENA signal ratio also increases with temperature (see Figure 4b). Furthermore, we find that the ratio of pairwise replacement to pairwise addition is higher for the Ir/TiO_2 catalyst compared to the Pt/TiO_2 catalyst and increases more rapidly with temperature for the Ir catalyst. We explored the branching between replacement and addition by changing the substrate properties while the catalyst and reaction conditions are kept the same. Experiments with p-H_2 using TFPE over TiO_2-supported Ir and Pt yielded strong ALTADENA signals on the fluoroalkene as well as the addition product, as seen in parts c and d of Figure 3, respectively. On both catalysts, substitution of methyl with trifluoromethyl resulted in lower conversion but increased pairwise replacement relative to pairwise reduction. The simultaneous reduction in conversion and relative increase in replacement can be explained in terms of lower adsorption enthalpy due to the strong electron-withdrawing trifluoromethyl group, as evidenced by the substantial chemical deshielding of the CH and CH_2 proton resonances. Removal of electron density from the π bond weakens adsorption.

Finally, we consider the mechanism underpinning the observation of hyperpolarized propene signals obtained by coadsorption of parahydrogen and propene (or trifluoropropene) on the Pt and Ir nanoparticle catalysts. As noted above, supported Pt and Ir particles facilitate deuteron exchange in any olefin, and in addition to alkanes, small amounts (up to 10%) of deuteroalkenes and HD are also generated. Incorporation of one or more deuterons into the alkene is explained by the HP mechanism. Can this sequential, stepwise hydrogen atom exchange preserve the spin correlation present in dihydrogen? This route is unlikely for two reasons: First, diffusion and comingling of H atoms on the surface will tend to randomize the adduct spin states resulting from a stepwise process, depending on surface properties and reaction conditions. Second, methyl rotation in the 2-propyl intermediate would

DOI: 10.1021/ja511476n
J. Am. Chem. Soc. 2015, 137, 1938–1946

likely randomize the cis and trans dispositions of the scalar order. This is inconsistent with the observed stereoselectivity of the pairwise replacement mechanism.

Next, we consider a hypothetical two-step process involving dehydrogenation of a gaseous propane intermediate, as proposed in the recent PASADENA study of the reaction of p-H_2 with propene-d_6:[28]

(i) propene + p-H_2 → propane**

(ii) propane** → propene** + H_2 (where ** indicates hyperpolarized scalar order).

In reference to the PASADENA spectrum shown in Figure 4b of ref 28, the enhanced propene CH_2 signals (H^b and H^c) exhibit similar intensities, and PHIP enhancement is observed on the CH_3 group (H^d). While these aspects are consistent with a propane** intermediate, cis−trans isomerization and double bond migration of surface propene**, mediated by the 2-propyl form, provide an alternative explanation. Since metal type and deuterium kinetic isotope effects play a significant role in reaction dynamics, we examined the two-step hypothesis for our catalysts, substrates, and reaction conditions in control studies. ALTADENA experiments were run with gas mixtures containing only propane and p-H_2 (with no propene) at the same reaction temperature and p-H_2 pressure that yielded strong propene ALTADENA signals. Propene formed by propane chemisorption could subsequently desorb, but it is much more likely to yield propane** by p-H_2 addition. Under our reaction conditions, such propane signals would be ∼10−20 times more intense than the propene** signals observed using propene in the reactant gas, yet the effluent contained no NMR-detectable propane** or propene**, as seen in Figure S6 in the Supporting Information. However, this negative result is unsurprising because dehydrogenation of alkanes over Pt is highly endothermic and is inhibited by preadsorbed H_2 and propene. Additionally, we performed ALTADENA experiments with varying propene partial pressures while the p-H_2 pressure and total flow rate were kept fixed. The propane dehydrogenation hypothesis requires propane to effectively compete with hydrogen and propene for surface adsorption sites. Figure 4c presents the propene partial pressure dependence of the propane** and propene** signals (spectra are shown in Figure S7, Supporting Information). Increasing the propene partial pressure should suppress propene** formation. To the contrary, we observe a monotonic increase in the propene** signals, ultimately saturating at the same pressure where the propane** signals also plateau. Additional evidence refuting the involvement of a propane** intermediate for our catalysts and reaction conditions is provided by the observed stereoselectivity of the disposition of the scalar order (see Figure 5a,c).

Next, we briefly consider a one-proton polarization mechanism, as reported in solution-state hydroformylation promoted by Pt−Sn and Ir carbonyl complexes.[44] This is deemed unlikely in view of the observed temperature activation of the SABRE-like process (Figure 4b).

Lastly, we consider a PR mechanism in which two H atoms of the alkene are replaced with two H atoms originating in the same H_2 molecule in a process that occurs entirely on the metal surface. In principle, this could occur in a concerted fashion, in which dehydrogenation and dihydrogen addition occur simultaneously (step V, Figure 6), or by a two-step process, in which sequential dehydrogenation is followed by pairwise rehydrogenation (steps VI + VII, Figure 6). The trend in the data shown in Figure 4c does not support a concerted path,

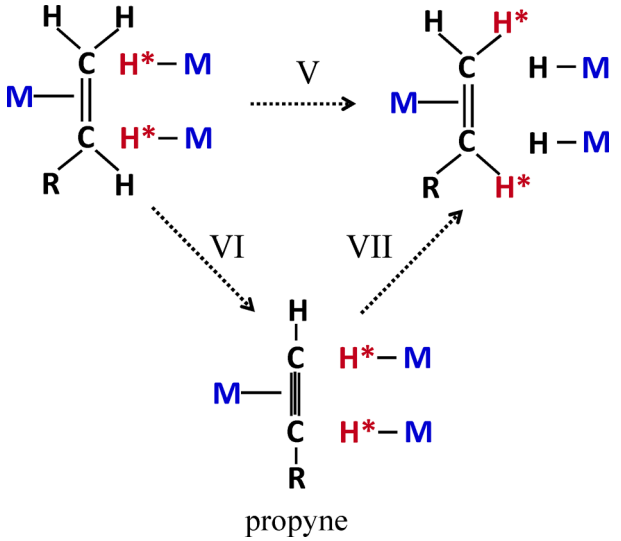

Figure 6. Double-replacement-state propene** yielding SABRE-like signals may be reached by a concerted process (step V) or by sequential dehydrogenation and pairwise rehydrogenation (steps V + VI).

because with decreasing propene pressure, the propene/propane signal ratio also decreases, suggesting that hyperpolarized propene is not a primary product. Furthermore, a concerted replacement reaction path would pass through a transition state with high entropic penalty and does not correspond to any known (or easily conceivable) elementary steps in catalysis. In contrast, dehydrogenation of alkenes on Pt and Ir is well-known and increases with temperature, consistent with the data presented in Figure 4b. Dehydrogenation can yield various C_3 structures, including propenylidene, propyne, and 1,2-propadiene, depending on the metal type and surface structure.[31] As a gaseous intermediate, propyne would be impossible to detect because the equilibrium (in excess H_2) favors propene/propane. Moreover, propyne is much more strongly adsorbed on metal surfaces than propene. Thus, a two-step path in which propene dehydrogenation is followed by pairwise rehydrogenation to propene** is deemed the most reasonable mechanism for the observed pairwise replacement. The pairwise rehydrogenation of propyne may be comparable to the direct saturation with a bound form of molecular p-H_2, possibly adsorbed onto low coordination metal atom sites, as described in the Introduction.

■ CONCLUSIONS

Supported metal catalysts were not expected to yield PHIP signals given the rapid diffusion of H atoms on the catalyst surface and in view of the sequential nature of the H atom addition in the HP mechanism. Symmetrization order is lost by randomization of spatial coordinates of H atoms. Hence, the discovery of PHIP signals using supported metal catalysts came as a surprise to many. Perhaps even more remarkably, supported Pt and Ir nanoparticles also catalyze pairwise replacement on propene and fluorinated propene, as demonstrated herein. By simply flowing a mixture of p-H_2 and substrate over the surface of the metal particles, symmetrization order is incorporated into the substrate without a change in its molecular structure, yielding intense PHIP/ALTADENA NMR signals. The observation of ALTADENA

DOI: 10.1021/ja511476n
J. Am. Chem. Soc. 2015, 137, 1938−1946

signals on Pt/SiO_2 and Pt/Al_2O_3 proves that pairwise replacement occurs at the metal particle surface.

By systematic variation of the reaction conditions, catalyst metal type, and chemical properties of the substrate, we have demonstrated that the PR-PHIP signals can be optimized, reaching levels as high as 40% relative to those resulting from pairwise addition. As a key methodology, we have shown how ALTADENA density matrix spectral simulations can provide information about the stereochemistry of hydrogenation, despite the complication of migration of the incipient scalar order under strong coupling conditions. The stereoselectivity indicates that the pairwise replacement process does not involve a surface-bound alkyl species, because the disposition of the hyperpolarized scalar order would be randomized in such an intermediate. A hypothetical mechanism involving dehydrogenation of hyperpolarized propane is also inconsistent with the observed stereoselectivity and is eliminated as a possibility by additional control studies. On the other hand, dehydrogenation of alkenes is facile on many metals (including Pt and Ir). Thus, pairwise replacement via a two-step dehydrogenation−rehydrogenation process (steps VI + VII in Figure 6) provides a reasonable explanation for the SABRE-like PR-PHIP signals.

Pairwise replacement has the potential to significantly broaden the scope of molecules that can be hyperpolarized by PHIP, though it is difficult to speculate on the extent of its generality. Further studies of this new polarization mechanism are motivated by the key advantages of supported metal particle catalysts over homogeneous and immobilized complexes. These advantages include higher stability, ease of separation from the catalyst, phase flexibility, compatibility with continuous-flow configuration, and adaptability to hyperpolarized MRI applications.

■ ASSOCIATED CONTENT

Supporting Information

Details of the catalyst synthesis, catalyst characterization, supplemental TEM micrographs and NMR spectra, and the formalism for the numerical density matrix spectra simulations. This material is available free of charge via the Internet at http://pubs.acs.org.

■ AUTHOR INFORMATION

Corresponding Author

bowers@chem.ufl.edu

Notes

The authors declare no competing financial interest.

■ ACKNOWLEDGMENTS

We thank William R. Dolbier, III, for generously providing 3,3,3-trifluoropropene and for helpful discussions, and Malcolm Levitt, for providing SpinDynamica two-spin ALTADENA simulation examples. We thank Dr. Katie Cychosz, Quantachrome Instruments, Boynton Beach, FL, for kindly performing H_2 and CO chemisorption measurements on our catalysts. Critical reading of the manuscript by Professor Daniel P. Weitekamp is gratefully acknowledged. The TEM work was carried out at Florida State University, and the TEM facility at FSU is funded and supported by the Florida State University Research Foundation, National High Magnetic Field Laboratory (NSF-DMR-0654118), and the State of Florida. Postdoc support from the University of Florida (to H.E.H.-W.) through startup funds is gratefully acknowledged. R.E.Q. acknowledges support from the NSF/NHMFL Summer REU program. This project was supported by ACS-PRF #52258-ND5.

■ REFERENCES

(1) Kurhanewicz, J.; Vigneron, D. B.; Brindle, K.; Chekmenev, E. Y.; Comment, A.; Cunningham, C. H.; DeBerardinis, R. J.; Green, G. G.; Leach, M. O.; Rajan, S. S.; Rizi, R. R.; Ross, B. D.; Warren, W. S.; Malloy, C. R. *Neoplasia* **2011**, *13*, 81−97.
(2) Bowers, C. R.; Weitekamp, D. P. *Phys. Rev. Lett.* **1986**, *57*, 2645−2648.
(3) Bowers, C. R.; Weitekamp, D. P. *J. Am. Chem. Soc.* **1987**, *109*, 5541−5542.
(4) Eisenschmid, T. C.; Kirss, R. U.; Deutsch, P. P.; Hommeltoft, S. I.; Eisenberg, R.; Bargon, J.; Lawler, R. G.; Balch, A. L. *J. Am. Chem. Soc.* **1987**, *109*, 8089−8091.
(5) Pravica, M. G.; Weitekamp, D. P. *Chem. Phys. Lett.* **1988**, *145*, 255−258.
(6) Eisenberg, R. *Acc. Chem. Res.* **1991**, *24*, 110−116.
(7) Bowers, C. R. In *Encyclopedia of Nuclear Magnetic Resonance*; Grant, D. M., Harris, R. K., Eds.; John Wiley & Sons, Ltd.: Chichester, UK, 2002; *Vol. 9*, p 750.
(8) Adams, R. W.; Aguilar, J. A.; Atkinson, K. D.; Cowley, M. J.; Elliott, P. I. P.; Duckett, S. B.; Green, G. G. R.; Khazal, I. G.; Lopez-Serrano, J.; Williamson, D. C. *Science* **2009**, *323*, 1708−1711.
(9) Duckett, S. B.; Sleigh, C. J. *Prog. Nucl. Magn. Reson. Spectrosc.* **1999**, *34*, 71−92.
(10) Hasnip, S. K.; Duckett, S. B.; Sleigh, C. J.; Taylor, D. R.; Barlow, G. K.; Taylor, M. J. *Chem. Commun. (Cambridge, U K)* **1999**, 1717−1718.
(11) Blazina, D.; Duckett, S. B.; Dunne, J. P.; Godard, C. *Dalton Trans.* **2004**, 2601−2609.
(12) Dunne, J. P.; Blazina, D.; Aiken, S.; Carteret, H. A.; Duckett, S. B.; Jones, J. A.; Poli, R.; Whitwood, A. C. *Dalton Trans.* **2004**, 3616−3628.
(13) Chekmenev, E. Y.; Hoevener, J.; Norton, V. A.; Harris, K.; Batchelder, L. S.; Bhattacharya, P.; Ross, B. D.; Weitekamp, D. P. *J. Am. Chem. Soc.* **2008**, *130*, 4212.
(14) Shchepin, R. V.; Coffey, A. M.; Waddell, K. W.; Chekmenev, E. Y. *J. Phys. Chem. Lett.* **2012**, *3*, 3281−3285.
(15) Cai, C.; Coffey, A. M.; Shchepin, R. V.; Chekmenev, E. Y.; Waddell, K. W. *J. Phys. Chem. B* **2013**, *117*, 1219−1224.
(16) Bhattacharya, P.; Chekmenev, E. Y.; Perman, W. H.; Harris, K. C.; Lin, A. P.; Norton, V. A.; Tan, C. T.; Ross, B. D.; Weitekamp, D. P. *J. Magn. Reson.* **2007**, *186*, 150−155.
(17) Barskiy, D. A.; Kovtunov, K. V.; Koptyug, I. V.; He, P.; Groome, K. A.; Best, Q. A.; Shi, F.; Goodson, B. M.; Shchepin, R. V.; Coffey, A. M.; Waddell, K. W.; Chekmenev, E. Y. *J. Am. Chem. Soc.* **2014**, *136*, 3322−3325.
(18) Skovpin, I. V.; Zhivonitko, V. V.; Kaptein, R.; Koptyug, I. V. *Appl. Magn. Reson.* **2013**, *44*, 289−300.
(19) Shi, F.; Coffey, A. M.; Waddell, K. W.; Chekmenev, E. Y.; Goodson, B. M. *Angew. Chem.* **2014**, *53*, 7495−7498.
(20) Kovtunov, K. V.; Zhivonitko, V. V.; Corma, A.; Koptyug, I. V. *J. Phys. Chem. Lett.* **2010**, *1*, 1705−1708.
(21) Skovpin, I. V.; Zhivonitko, V. V.; Koptyug, I. V. *Appl. Magn. Reson.* **2011**, *41*, 393−410.
(22) Koptyug, I. V.; Kovtunov, K. V.; Burt, S. R.; Anwar, M. S.; Hilty, C.; Han, S.-I.; Pines, A.; Sagdeev, R. Z. *J. Am. Chem. Soc.* **2007**, *129*, 5580−5586.
(23) Kovtunov, K. V.; Beck, I. E.; Bukhtiyarov, V. I.; Koptyug, I. V. *Angew. Chem. Int. Ed* **2008**, *47*, 1492−1495.
(24) Zhivonitko, V. V.; Kovtunov, K. V.; Beck, I. E.; Ayupov, A. B.; Bukhtiyarov, V. I.; Koptyug, I. V. *J. Phys. Chem. C* **2011**, *115*, 13386−13391.
(25) Salnikov, O. G.; Kovtunov, K. V.; Barskiy, D. A.; Bukhtiyarov, V. I.; Kaptein, R.; Koptyug, I. V. *Appl. Magn. Reson.* **2013**, *44*, 279−288.
(26) Kovtunov, K. V.; Zhivonitko, V. V.; Skovpin, I. V.; Barskiy, D. A.; Koptyug, I. V. *Top. Curr. Chem.* **2013**, *338*, 123−180.

DOI: 10.1021/ja511476n
J. Am. Chem. Soc. 2015, 137, 1938−1946

(27) Kovtunov, K. V.; Zhivonitko, V. V.; Skovpin, I. V.; Barskiy, D. A.; Salnikov, O. G.; Koptyug, I. V. *J. Phys. Chem. C* **2013**, *117*, 22887−22893.
(28) Kovtunov, K. V.; Truong, M. L.; Barskiy, D. A.; Salnikov, O. G.; Bukhtiyarov, V. I.; Coffey, A. M.; Waddell, K. W.; Koptyug, I. V.; Chekmenev, E. Y. *J. Phys. Chem. C* **2014**, *118*, 28234−28243.
(29) Kovtunov, K. V.; Barskiy, D. A.; Coffey, A. M.; Truong, M. L.; Salnikov, O. G.; Khudorozhkov, A. K.; Inozemtseva, E. A.; Prosvirin, I. P.; Bukhtiyarov, V. I.; Waddell, K. W.; Chekmenev, E. Y.; Koptyug, I. V. *Chem.—Eur. J.* **2014**, *20*, 11636−11639.
(30) Horiuti, I.; Polanyi, M. *Trans. Faraday Soc.* **1934**, *30*, 1164−1172.
(31) Bond, G. C. *Metal-Catalysed Reactions of Hydrocarbons*; Springer Science: New York, 2005.
(32) Bond, G. C.; Phillips, J. J.; Winterbottom, J. M.; Wells, P. B. *Trans. Faraday Soc.* **1964**, *60*, 1847−1864.
(33) Yang, B.; Gong, X. Q.; Wang, H. F.; Cao, X. M.; Rooney, J. J.; Hu, P. *J. Am. Chem. Soc.* **2013**, *135*, 15244−15250.
(34) Vile, G.; Baudouin, D.; Remediakis, I. N.; Coperet, C.; Lopez, N.; Perez-Ramirez, J. *ChemCatChem.* **2013**, *5*, 3750−3759.
(35) Kovtunov, K. V.; Beck, I. E.; Zhivonitko, V. V.; Barskiy, D. A.; Bukhtiyarov, V. I.; Koptyug, I. V. *Phys. Chem. Chem. Phys.* **2012**, *14*, 11008−11014.
(36) Tauster, S. J. *Acc. Chem. Res.* **1987**, *20*, 389−394.
(37) Cremer, P. S.; Su, X. C.; Shen, Y. R.; Somorjai, G. A. *J. Phys. Chem.* **1996**, *100*, 16302−16309.
(38) Bus, E.; van Bokhoven, J. A. *Phys. Chem. Chem. Phys.* **2007**, *9*, 2894−2902.
(39) Loane, R. F.; Xu, P. R.; Silcox, J. *Acta Crystallogr., Sect. A* **1991**, *47*, 267−278.
(40) Pennycook, S. J.; Boatner, L. A. *Nature* **1988**, *336*, 565−567.
(41) Rasband, W. S. *ImageJ*; U.S National Institutes of Health: Bethesda, MD, 1997−2014 (http://imagej.nih.gov/ij/).
(42) Due to miscalibration of the RF field; a 90° pulse was intended.
(43) Levitt, M. H.; Rantaharju, J.; Brinkmann, A. www.SpinDynamica.soton.ac.uk.
(44) Permin, A. B.; Eisenberg, R. *J. Am. Chem. Soc.* **2002**, *124*, 12406−12407.

DOI: 10.1021/ja511476n
J. Am. Chem. Soc. 2015, 137, 1938−1946